Characterization and Performance Improvement of Cooperative Wireless Networks with Nonlinear Power Amplifier at Relay

Mahdi Majidi, *Member, IEEE,* Abbas Mohammadi, *Senior Member, IEEE,* Abdolali Abdipour, *Senior Member, IEEE,* and Mikko Valkama, *Senior Member, IEEE*

***Abstract*—In this paper, the performance of the cooperative cognitive radio network with the amplify-and-forward protocol is studied when the relay uses a nonlinear power amplifier (NLPA). Furthermore, taking the pulse shaping filter for the data signal into account, the power of the adjacent channel interference (ACI) to the primary users (PUs) caused by the spectral regrowth of the relay output signal is analytically calculated. Moreover, two compensation techniques are proposed which are implemented at the destination receiver to deal with the in-band nonlinear interference. The first technique is based on the calculation of the distorted signal constellation to enhance the performance of the demodulator. The second technique is feedforward compensation at the receiver. The bit error rate (BER) expressions for both techniques are presented. The ACI resulting from the spectral regrowth due to the relay NLPA is investigated by the simulation and numerical studies, and then, the BER performance degradation at the destination node and the performance improvement resulting from the proposed compensation methods are evaluated. Since the ACI confines the transmit power due to the interference power constraint of the PU, the achievable BER of the secondary user (SU) is studied. The simulation results show that the feedforward compensation technique has better BER performance than the modified constellation based approach.**

***Index Terms*—Amplify and forward, power amplifier nonlinearity, cognitive radio, maximum ratio combining, nonlinearity compensation.**

I. Introduction

Cooperative communications, which is considered as a promising technique for next generation wireless networks, show great advantages in offering high transmission capacity and reliability, network coverage, and quality of service [1], [2]. The classification of the cooperative schemes depends on the procedures used by the relay to process the received signal from the source [3]. One of the most common relaying schemes is amplify-and-forward (AF) protocol that simply amplifies and transmits the received signal without any further processing. Hence, it has low latency and complexity [4]. Although noise is amplified by the relay too, the AF method can achieve full diversity order by using two independently faded versions of the signal at the destination [5], [6]. In this paper, we adopt the AF protocol.

In general, the power amplifier (PA) is one crucial element of any radio transmitter and consumes a large portion of energy [7]. In many works, this analog component is assumed to operate in linear region to make the performance analysis more straightforward. However, PAs indeed have nonlinear behavior, particularly when they operate at medium to high power levels [8]. The nonlinearity of the PA causes both in-band and out-of-band distortions. The former distortion increases the bit error rate (BER) of transmission and degrades the system capacity. The latter distortion which follows from the spectral regrowth of the PA output signal results in interference to the receivers that are using the adjacent channels which is called adjacent channel interference (ACI) [9]. PA linearity and efficiency are generally two conflicting requirements such that more efficient PAs usually introduce more distortions [10]. Linearization techniques can be employed to mitigate these impairments [11], however, nonlinear distortion effects cannot be totally eliminated at the RF level [12]. Moreover, most of the methods are complex and consume energy, and hence, cannot be implemented in resource-constrained devices such as relays [4]. Accordingly, the nonlinear distortion effects are more pronounced in relays [13]. In the context of cognitive radio (CR) network, the secondary user (SU) should keep the interference power at the primary users (PUs) below a predefined interference power constraint [14], [15]. This constraint, when the relay in the CR network has a nonlinear PA (NLPA), results in the limitation of the transmit power, and consequently, degrades the SU performance [16]. One of the applications of cooperation in CR networks is to increase diversity in SU communication [17], [18]. A survey on various methods of resource allocation in cooperative cognitive radio networks is presented in [19]. In [20], [21], by taking into account linear interference from source and relays of CR network into PUs, the resource allocation and optimization are perused, but so far, the nonlinear distortion effect of the NLPA in the cooperative CR network have not been investigated.

In general, when the input signal to the NLPA is of OFDM type, it can be assumed that it has Gaussian distribution and according to the Bussgang theorem, the nonlinear distortion at the output of the receiver FFT can be considered as the summation of an additive Gaussian noise and the input signal scaled by a complex factor [22], [23], which makes the analytical evaluation of the system performance more

M. Majidi is with the Department of Electrical and Computer Engineering, University of Kashan, Kashan, Iran (e-mail: m.majidi@kashanu.ac.ir).

A. Mohammadi and A. Abdipour are with the Department of Electrical Engineering, Amirkabir University of Technology, Tehran 15875-4413, Iran (e-mail: {abm125,abdipour}@aut.ac.ir).

M. Valkama is with the Department of Electronics and Communications Engineering, Tampere University of Technology, Tampere, Finland (e-mail: mikko.e.valkama@tut.fi).

straightforward. For the AF protocol with NLPA at relay, combined with OFDM modulation, error and outage probabilities are reported in [24]–[26], performance analysis of relay selection is carried out in [27] and [28], and methods for power allocation and modification of coefficients of the maximum ratio combining (MRC) at the receiver are developed in [4]. In order to compensate the effect of NLPA at relay in an OFDM based AF network, in [29], a feedback procedure is used in receiver to eliminate the additive noise produced due to the nonlinear distortion from relay, however, this method increases the delay because of the feedback loop. In the literature, the ACI resulting from NLPA at the relay which is an important aspect in CR networks has not been investigated.

The work in [30] considers an AF system with limited power and non-OFDM based modulation, and thus, is not building on the simplifying Gaussian input signal assumption anymore. In that work, MRC weights have been obtained, however, the impact of pulse shape and matched filter (MF) at the destination receiver are not considered. Similarly, in [2], the average signal-to-noise ratio (SNR) and symbol error rate at destination are computed when the input signal is not Gaussian distributed and there is third order nonlinearity at the output of the relay PA. However, the MRC weights are not modified and the MF at the destination is ignored in the analysis. Because of spectral regrowth of the relay output due to the third order distortion, if it is assumed that there is no MF at the destination which limits the bandwidth, the input bandwidth at destination should be three times the input signal bandwidth at source which is not practical. On the other hand, when NLPA is used in relay transmission, even though the effective pulse shape is Nyquist, the output of the MF includes intersymbol interference (ISI) which should be taken into account. It is worth noting that in the literature related to cooperative communications with NLPA at the relay, the resulting spectral regrowth and the ACI to the PUs which are very important aspects in CR networks have not been investigated.

This paper investigates a cooperative AF system for non-Gaussian distributed source signal, where the source and relay nodes have linear and nonlinear PA, respectively, and the destination has a filter matched to the signal pulse shape. First, the PSD of the relay output in terms of its input SNR is derived. Then, the interference level to the adjacent channels of the relay is analytically calculated which forms a valuable result for interference management in the CR network. At destination, MRC is utilized to combine the received signals from source and relay. By awareness of the nonlinear behavioral model of the relay PA, we then present two techniques at the destination for reducing the nonlinear distortion effects. First, for an arbitrary linear digital modulation, the resulting distorted signal constellation after the combination of two branches at the destination is derived which can be employed to modify the decision regions for detection of the data symbols. In the second technique which is called feedforward compensation, the destination uses the received signal from the source to reconstruct and eliminate the nonlinear distortion of the received signal from the relay. A polynomial model with arbitrary order of nonlinearity is assumed for the NLPA in the two proposed techniques. Furthermore, for both methods, we redesign the weights used in MRC with respect to the noise power and nonlinear distortion levels. Specifically, the main contributions of this paper can be summarized as follows:

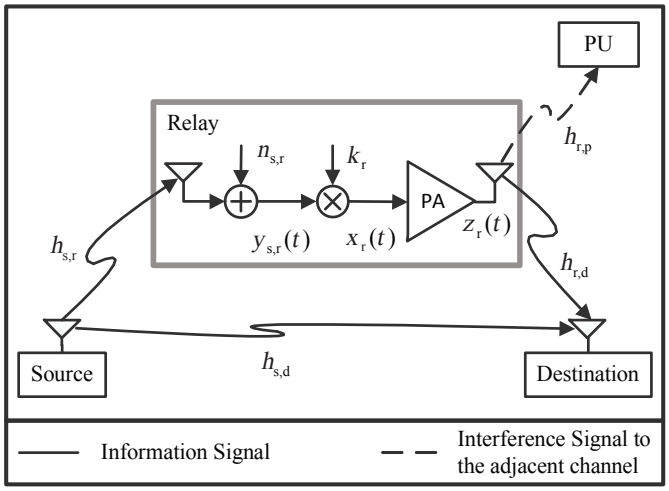

Fig. 1. An AF cooperative cognitive network with an NLPA at the relay node.

- Analytically formulating the spectral leakage at the relay when its PA is nonlinear.
- Nonlinear compensation of the relay NLPA at the destination of an AF cooperative network by the feedforward technique and estimation of the distorted signal constellation.
- Redesign of the MRC weights for both proposed compensation techniques.
- Providing the theoretical BER expressions for the proposed compensation techniques.
- Extensive set of empirical numerical results are provided, showing the accuracy of the analytical results.

The rest of this paper is organized as follows: Section II introduces the system and channel models. Section III derives the spectral leakage due to the PA nonlinearity at the relay and presents the adjacent channel power analysis. In Section IV two compensation schemes at the destination are proposed, and the MRC weights are analytically calculated for both of them. The probabilities of error of the suggested compensation methods are derived in Section V. Numerical results and discussion are provided in Section VI. Finally, Section VII summarizes the main findings.

II. System and Channel Models

We consider a two-hop single-relay network as illustrated in Fig. 1 which consists of one source, one relay, and one destination. By considering AF protocol, in the first time slot, the source broadcasts its signal to the relay and destination by using a linear PA. In the second time slot, the relay forwards the received signal to the destination with an NLPA. As shown in Fig. 1, four flat fading channels involved in this system are the source-destination, source-relay, relay-destination, and relay-PU, which are mutually independent and denoted by $h_{\mathrm{s,d}}$, $h_{\mathrm{s,r}}$, $h_{\mathrm{r,d}}$, and $h_{\mathrm{r,p}}$, respectively. In the following, the transmit and receive signals at the nodes will be described.

A. Source Node

The data signal at source is given by

$$x_{\rm s}(t) = \sum_{n=-\infty}^{+\infty} s_n g(t-nT), \tag{1}$$

where s_n is the nth data symbol, T is the symbol duration, and $g(t)$ is a band-limited pulse shaping filter with bandwidth B such that $B \leqslant 1/T$. The data symbols are assumed to be zero mean, independent and identically distributed (i.i.d.) as well as symmetric complex random variables (such as square M-QAM) with unit variance. Before transmission, $x_{\rm s}(t)$ will be scaled by $\sqrt{P_{\rm s}}$ which makes the power of the resulting signal to be $P_{\rm s}\mathcal{E}_g/T$ where $\mathcal{E}_g$ is the energy of $g(t)$ [31]. Finally, it is amplified by a linear PA with coefficient a_1, and hence, the signal $a_1\sqrt{P_{\rm s}}x_{\rm s}(t)$ is transmitted from the source.

B. Relay Node

The received signal at the relay node is given by

$$y_{\rm s,r}(t) = h_{\rm s,r}a_1\sqrt{P_{\rm s}}x_{\rm s}(t) + n_{\rm s,r}(t), \tag{2}$$

where $n_{\rm s,r}(t)$ is the additive circularly symmetric complex Gaussian noise process. We assume that there is an ideal low-pass filter with bandwidth B at the input of the relay. Hence, the power spectral density (PSD) of the noise is equal to $N_0\Pi(\frac{f}{2B})$ where $\Pi(f)$ is a rectangular function which takes the value 1 for $|f| \leq 0.5$, and zero otherwise. Therefore, the noise power at the relay, denoted by $\sigma^2_{n_{\rm s,r}}$, is $2N_0B$. As shown in Fig. 1, the received signal $y_{\rm s,r}(t)$ is scaled by $k_{\rm r}$ to provide the input signal of the relay PA as follows

$$\begin{aligned} x_{\rm r}(t) &= k_{\rm r}y_{\rm s,r}(t) \\ &= k_{\rm r}h_{\rm s,r}a_1\sqrt{P_{\rm s}}x_{\rm s}(t) + k_{\rm r}n_{\rm s,r}(t), \end{aligned} \tag{3}$$

where $k_{\rm r}$ is determined such that the power of $x_{\rm r}(t)$ is $P_{\rm r}\mathcal{E}_g/T$ and $P_{\rm r}$ is the power scaling factor. Hence, we have

$$k_{\rm r} = \frac{\sqrt{P_{\rm r}\mathcal{E}_g/T}}{\sqrt{|h_{\rm s,r}|^2\,|a_1|^2\,P_{\rm s}\mathcal{E}_g/T + 2N_0B}}, \tag{4}$$

where the denominator is the square root of the power of $y_{\rm s,r}(t)$. For the NLPA at the relay, we adopt the $(2N_p+1)$th-order nonlinear behavioural model of the form [32]–[34]

$$z_{\rm r}(t) = \sum_{i=0}^{N_p} a_{2i+1}x_{\rm r}(t)\,|x_{\rm r}(t)|^{2i}, \tag{5}$$

where $z_{\rm r}(t)$ is the output signal of the PA transmitted for the destination node, and the coefficients a_{2i+1} can be complex in general. Using (2) and (3), we can write $z_{\rm r}(t)$ as (6) on the bottom of this page where $x^{\rm NL}_{\rm s}(t)$ contains different powers of $x_{\rm s}(t)$ as follows

$$x^{\rm NL}_{\rm s}(t) \triangleq \sum_{i=1}^{N_p} a_{2i+1}k_{\rm r}^{2i+1}\left(h_{\rm s,r}a_1\sqrt{P_{\rm s}}x_{\rm s}(t)\right)\left|h_{\rm s,r}a_1\sqrt{P_{\rm s}}x_{\rm s}(t)\right|^{2i}, \tag{7}$$

and $w_{\rm r,d}(t)$ is the summation of all cross-multiplication terms of the various powers of signal $x_{\rm s}(t)$ and noise $n_{\rm s,r}(t)$ in (6).

C. Destination Node

The received signals at the destination node in the first and second time slots from the source and relay nodes, respectively, are given by

$$y_{\rm s,d}(t) = h_{\rm s,d}a_1\sqrt{P_{\rm s}}x_{\rm s}(t) + n_{\rm s,d}(t) \tag{8}$$

$$y_{\rm r,d}(t) = h_{\rm r,d}z_{\rm r}(t) + n_{\rm r,d}(t), \tag{9}$$

where the noise processes $n_{\rm s,d}(t)$ and $n_{\rm r,d}(t)$ have the same distribution as $n_{\rm s,r}(t)$ in (2). Using (6), the received signal from the relay can be written in terms of the data signal as follows

$$\begin{aligned} y_{\rm r,d}(t) =& h_{\rm s,r}h_{\rm r,d}k_{\rm r}a_1^2\sqrt{P_{\rm s}}x_{\rm s}(t) + h_{\rm r,d}k_{\rm r}a_1n_{\rm s,r}(t) + n_{\rm r,d}(t) \\ &+ h_{\rm r,d}\left(x^{\rm NL}_{\rm s}(t) + w_{\rm r,d}(t)\right), \end{aligned} \tag{10}$$

where the NLPA at the relay accounts for the last term.

D. PU Node

In the system model, shown in Fig. 1, the CR system, including source, relay, and destination nodes performs data transmission in a spectrum hole. However, the nonlinearity of the PA at the relay results in spectral leakage to the adjacent channel, and hence, introduces interference to the PU node. In the CR network, the power of this interference, denoted by $P_{\rm AC}$, must be smaller than a predefined maximum tolerable interference power, represented by Q, as follows

$$P_{\rm AC} \leq Q, \tag{11}$$

where $P_{\rm AC}$ is calculated in the next section.

III. Spectral Leakage Analysis

The spectral leakage resulting from the NLPA at the relay causes interference to the adjacent channels. In addition, in the CR network, the interferences from the secondary transmitters (STs) to the PUs have to be controlled. In order to compute the ACI, the PSD of the PA output signal is needed. Without loss

$$z_{\rm r}(t) = h_{\rm s,r}k_{\rm r}a_1^2\sqrt{P_{\rm s}}x_{\rm s}(t) + k_{\rm r}a_1n_{\rm s,r}(t) + \underbrace{\sum_{i=1}^{N_p} a_{2i+1}k_{\rm r}^{2i+1}\left(h_{\rm s,r}a_1\sqrt{P_{\rm s}}x_{\rm s}(t) + n_{\rm s,r}(t)\right)\left|h_{\rm s,r}a_1\sqrt{P_{\rm s}}x_{\rm s}(t) + n_{\rm s,r}(t)\right|^{2i}}_{\triangleq\, x^{\rm NL}_{\rm s}(t) + w_{\rm r,d}(t)}. \tag{6}$$

TABLE I
THE PARAMETERS β_{mn}.

	Definition		Definition
β_{11}	$k_{\rm r}^2 \left\|h_{\rm s,r}\right\|^2 \left\|a_1\right\|^4 P_{\rm s}$	β_{13}	$a_1 a_3^* k_{\rm r}^4 \left\|h_{\rm s,r}\right\|^4 \left\|a_1\right\|^4 P_{\rm s}^2$
β_{22}	$k_{\rm r}^2 \left\|a_1\right\|^2$	β_{18}	$2a_1 a_3^* k_{\rm r}^4 \left\|h_{\rm s,r}\right\|^2 \left\|a_1\right\|^2 P_{\rm s}$
β_{33}	$\left\|a_3\right\|^2 k_{\rm r}^6 \left\|h_{\rm s,r}\right\|^6 \left\|a_1\right\|^6 P_{\rm s}^3$	β_{26}	$a_1 a_3^* k_{\rm r}^4$
β_{44}	$\left\|a_3\right\|^2 k_{\rm r}^6 \left\|h_{\rm s,r}\right\|^4 \left\|a_1\right\|^4 P_{\rm s}^2$	β_{27}	$2a_1 a_3^* k_{\rm r}^4 \left\|h_{\rm s,r}\right\|^2 \left\|a_1\right\|^2 P_{\rm s}$
β_{55}	$\left\|a_3\right\|^2 k_{\rm r}^6 \left\|h_{\rm s,r}\right\|^2 \left\|a_1\right\|^2 P_{\rm s}$	β_{38}	$2\left\|a_3\right\|^2 k_{\rm r}^6 \left\|h_{\rm s,r}\right\|^4 \left\|a_1\right\|^4 P_{\rm s}^2$
β_{66}	$\left\|a_3\right\|^2 k_{\rm r}^6$	β_{67}	$2\left\|a_3\right\|^2 k_{\rm r}^6 \left\|h_{\rm s,r}\right\|^2 \left\|a_1\right\|^2 P_{\rm s}$
β_{77}	$4\left\|a_3\right\|^2 k_{\rm r}^6 \left\|h_{\rm s,r}\right\|^4 \left\|a_1\right\|^4 P_{\rm s}^2$		
β_{88}	$4\left\|a_3\right\|^2 k_{\rm r}^6 \left\|h_{\rm s,r}\right\|^2 \left\|a_1\right\|^2 P_{\rm s}$		

of generality, we calculate the PSD for a third-order NLPA. First, $z_{\rm r}(t)$ from (5) is rewritten as

$$\begin{aligned} z_{\rm r}(t) = {} & k_{\rm r} h_{\rm s,r} a_1^2 \underbrace{\sqrt{P_{\rm s}} x_{\rm s}(t)}_{1} + k_{\rm r} a_1 \underbrace{n_{\rm s,r}(t)}_{2} + a_3 k_{\rm r}^3 \Big\{ h_{\rm s,r} a_1 \\ & \left|h_{\rm s,r} a_1\right|^2 P_{\rm s}^{\frac{3}{2}} \underbrace{x_{\rm s}^2(t) x_{\rm s}^*(t)}_{3} + h_{\rm s,r}^2 a_1^2 P_{\rm s} \underbrace{x_{\rm s}^2(t) n_{\rm s,r}^*(t)}_{4} \\ & + h_{\rm s,r}^* a_1^* \sqrt{P_{\rm s}} \underbrace{x_{\rm s}^*(t) n_{\rm s,r}^2(t)}_{5} + \underbrace{n_{\rm s,r}(t) \left|n_{\rm s,r}(t)\right|^2}_{6} + 2\left|h_{\rm s,r} a_1\right|^2 \\ & P_{\rm s} \underbrace{\left|x_{\rm s}(t)\right|^2 n_{\rm s,r}(t)}_{7} + 2 h_{\rm s,r} a_1 \sqrt{P_{\rm s}} \underbrace{x_{\rm s}(t) \left|n_{\rm s,r}(t)\right|^2}_{8} \Big\}. \end{aligned} \tag{12}$$

where $(.)^*$ denotes the complex conjugate. The autocorrelation function of the cyclostationary process $z_{\rm r}(t)$ which can be calculated by $\mathrm{E}\left\{z_{\rm r}(t) z_{\rm r}^*(t+\tau)\right\}$ reads as follows

$$R_{2z_{\rm r}}(t;\tau) = \sum_{m=1}^{8} \sum_{n=1}^{8} \beta_{mn} R_{2z_{\rm r}}^{(m,n)}(t;\tau), \tag{13}$$

where $R_{2z_{\rm r}}^{(m,n)}(t;\tau)$ is the cross-correlation function between the mth term of $z_{\rm r}(t)$ in (12) and the nth term of $z_{\rm r}(t+\tau)$, and the coefficients β_{mn} are given in Table I. Regarding the coefficients on the right side of the table we have $\beta_{mn} = \beta_{nm}^*$, and some parameters β_{mn} which are not defined in the table are zero because of two reasons; First, according to a moment theorem from [35] stated in Appendix A for zero mean complex Gaussian noise, if the number of conjugated elements are not equal to the others, the moment is zero. Secondly, since the data signal constellation is assumed to be complex symmetric the odd order moments of $x_{\rm s}(t)$ are equal to zero [36]. We have to extract non-zero $R_{2z_{\rm r}}^{(m,n)}(t;\tau)$ in terms of autocorrelation of noise and joint cumulants of $x_{\rm s}(t)$ which can be done by employing Leonov-Shiryaev formula [37], [38]. In order to demonstrate this method, the derivation of $R_{2z_{\rm r}}^{(7,7)}(t;\tau)$ is provided in Appendix B which results in

$$\begin{aligned} R_{2z_{\rm r}}^{(7,7)}(t;\tau) = {} & \Big\{ C_{2x_{\rm s}}(t;0^*) C_{2x_{\rm s}}(t+\tau;0^*) + \left|C_{2x_{\rm s}}(t;\tau^*)\right|^2 \\ & + C_{4x_{\rm s}}(t;0^*,\tau,\tau^*) \Big\} R_{n_{\rm s,r}}(\tau), \end{aligned} \tag{14}$$

where $R_{n_{\rm s,r}}(\tau)$ is the autocorrelation function of $n_{\rm s,r}(t)$ and $C_{kx_{\rm s}}$ is the kth-order cumulant of $x_{\rm s}(t)$ and the τ^* in its argument implies that the corresponding term, $x_{\rm s}(t+\tau)$, is conjugated. For instance, $C_{4x_{\rm s}}(t;0^*,\tau,\tau^*) = \mathrm{cum}\left\{x_{\rm s}(t), x_{\rm s}^*(t), x_{\rm s}(t), x_{\rm s}^*(t+\tau)\right\}$ where $\mathrm{cum}\left\{\cdot\right\}$ denotes the cumulant operation [39]. We can rewrite each joint cumulant in (14) as $c_{i+n,x_{\rm s}}(t;\tau)_q$ where $i+n$ is the order of cumulant, n is the number of terms of cumulant with lag τ, and q denotes the number of terms which are complex conjugate, for example, $C_{4x_{\rm s}}(t;0^*,\tau,\tau^*) = c_{2+2,x_{\rm s}}(t;\tau)_2$. Now we have the autocorrelation function $R_{2z_{\rm r}}(t;\tau)$ and we need its time average in order to compute the PSD. Hence, the kth order joint cumulant of $x_{\rm s}(t)$ in form of separate t-dependent and τ-dependent functions is needed which is given in [39] as

$$c_{i+n,x_{\rm s}}(t;\tau)_q = \frac{\gamma_{s,i+n,q}}{T} \sum_{m=-\infty}^{+\infty} \rho_{\frac{m}{T}}^{(i,n)}(\tau) \mathrm{e}^{\frac{-j2\pi}{T} m t}, \tag{15}$$

where $\gamma_{s,k,q}$ is the kth-order cumulant with q conjugations of the data symbols s_n, and $\rho_u^{(i,n)}(\tau)$ for every u is defined as

$$\rho_u^{(i,n)}(\tau) \triangleq \int_{-\infty}^{+\infty} G_i(f+u) G_n(f) \mathrm{e}^{j2\pi f \tau} df, \tag{16}$$

where $G_i(f) \triangleq F\{g^i(t)\}$ and $F\{\cdot\}$ denotes the Fourier transform. Using (15), we can rewrite $R_{2z_{\rm r}}(t;\tau)$ and integrate over the period T to obtain its time average $R_{2z_{\rm r}}(\tau)$ as follows

$$R_{2z_{\rm r}}(\tau) = \sum_{m=1}^{8} \sum_{n=1}^{8} \beta_{mn} R_{2z_{\rm r}}^{(m,n)}(\tau), \tag{17}$$

where $R_{2z_{\rm r}}^{(m,n)}(\tau)$ is the time average of $R_{2z_{\rm r}}^{(m,n)}(t;\tau)$. For instance, the time average of $R_{2z_{\rm r}}^{(7,7)}(t;\tau)$ from (14) is calculated as follows

$$\begin{aligned} R_{2z_{\rm r}}^{(7,7)}(\tau) = {} & \Bigg\{ \left(\frac{\gamma_{\rm s,2,1}}{T}\right)^2 \sum_{m=-1}^{1} \left(\rho_{\frac{m}{T}}^{(1,1)}(0)\right)^2 \mathrm{e}^{(\frac{-j2\pi}{T} m\tau)} + \\ & \left(\frac{\gamma_{\rm s,2,1}}{T}\right)^2 \sum_{m=-1}^{1} \rho_{\frac{m}{T}}^{(1,1)}(\tau) \rho_{\frac{-m}{T}}^{(1,1)}(\tau) + \frac{\gamma_{\rm s,4,2}}{T} \rho_0^{(2,2)}(\tau) \Bigg\} R_{n_{\rm s,r}}(\tau). \end{aligned} \tag{18}$$

Finally, the PSD of $z_{\rm r}(t)$ which is the Fourier transform of $R_{2z_{\rm r}}(\tau)$ becomes

$$S_{2z_{\rm r}}(f) = \sum_{m=1}^{8} \sum_{n=1}^{8} \beta_{mn} S_{2z_{\rm r}}^{(m,n)}(f), \tag{19}$$

where for example $S_{2z_{\rm r}}^{(7,7)}(f)$ reads as follows

$$\begin{aligned} S_{2z_{\rm r}}^{(7,7)}(f) = {} & \Bigg\{ \left(\frac{\gamma_{\rm s,2,1}}{T}\right)^2 \sum_{m=-1}^{1} \left(\rho_{\frac{m}{T}}^{(1,1)}(0)\right)^2 \delta\left(f - \frac{m}{T}\right) \\ & + \left(\frac{\gamma_{\rm s,2,1}}{T}\right)^2 \sum_{m=-1}^{1} \left(G\left(f + \frac{m}{T}\right) G(f)\right) \star \left(G\left(f - \frac{m}{T}\right) G(f)\right) \\ & + \frac{\gamma_{\rm s,4,2}}{T} G_2^2(f) \Bigg\} \star \left\{ N_0 \Pi\left\{\frac{f}{2B}\right\} \right\}, \end{aligned} \tag{20}$$

where $G(f) \triangleq F\{g(t)\}$, $\Pi(f)$ and $\delta(f)$ are the rectangular and Dirac delta functions, respectively, and $\star$ denotes the convolution operation.

The SNR at the relay in a block fading is given by

$$\mathrm{SNR}_{\rm r} = \frac{\left|h_{\rm s,r}\right|^2 \left|a_1\right|^2 P_{\rm s} \mathcal{E}_g}{2 N_0 B T}. \tag{21}$$

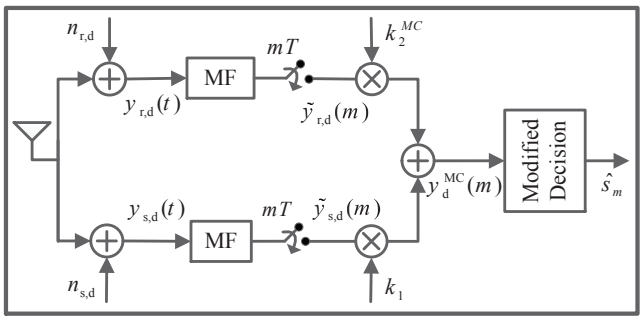

(a)

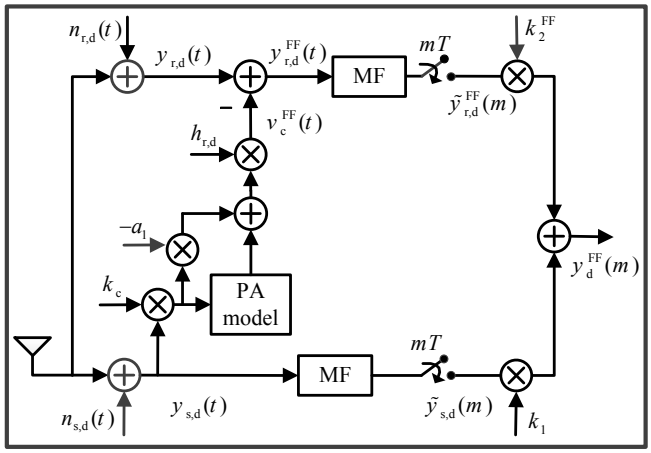

(b)

Fig. 2. Two methods for compensation of the PA nonlinearity, (a) Modified decision regions and MRC coefficients, (b) Feedforward method with modified MRC weights.

As mentioned in Section II-B, the power of the input signal to the PA of relay is set to $P_{\rm r}\mathcal{E}_g/T$, however, the changes of $\mathrm{SNR_r}$ due to the changes of the fading channel $h_{\rm s,r}$, causes the PSD of the relay output signal to be different at the various realizations of $h_{\rm s,r}$. This issue will be investigated in Section VI.

In the CR network context, the ACP (adjacent channel power) resulting from the spectral regrowth of the relay output should be controlled. The ACP in the adjacent channel with frequency limits f_1 and f_2 is obtained by integrating $S_{2z_{\rm r}}(f)$ over that interval, and then, taking the statistical expectation over $h_{\rm r,p}$ as follows

$$P_{\rm AC} = \mathrm{E}_{h_{\rm r,p}} \left\{ \int_{f_1}^{f_2} S_{2z_{\rm r}}(f) df \right\}, \tag{22}$$

which depends on $P_{\rm s}$ and $P_{\rm r}$.

IV. Compensation of the PA Nonlinearity at the Destination

In this section, the effects of the NLPA at the relay on the detected signal at the receiver node are examined and two compensation methods are presented. Fig. 2(a) illustrates the block diagram of the receiver node using the MRC method. We assume that the channel state information of all fading channels and the PA models of the source and relay nodes are available at the destination. It is worth mentioning that when a transmitter uses NLPA, the training sequence that can be used at the receiver for channel estimation is the transmitter's training sequence which is passed through the NLPA model, and as a result, the estimation would be straightforward. The impulse response of the MF is the mirror-image of the pulse shaping filter of the transmitter, i.e., $g(-t)$, and with the assumption of even symmetry it equals $g(t)$. For any signal $y(t)$, we define $\tilde{y}(m)$ as

$$\tilde{y}(m) \triangleq \int_{-\infty}^{+\infty} y(t) g(t - mT) dt. \tag{23}$$

Using (1) and (8), the received signal at the source node, $y_{\rm s,d}(t)$, after passing through the MF and sampling at time mT is given by

$$\tilde{y}_{\rm s,d}(m) = h_{\rm s,d} a_1 \sqrt{P_{\rm s}} \mathcal{E}_g s_m + \tilde{n}_{\rm s,d}(m), \tag{24}$$

where in order to avoid ISI between the samples $\tilde{y}_{\rm s,d}(m)$, we assume that the effective pulse shape $g(t) \star g(t)$ satisfies the Nyquist criterion [31] [40, p. 145]. Similarly, $y_{\rm r,d}(t)$ from (10) after passing through the MF and sampling is given by

$$\begin{aligned} \tilde{y}_{\rm r,d}(m) = & h_{\rm s,r} h_{\rm r,d} k_{\rm r} a_1^2 \sqrt{P_s} \mathcal{E}_g s_m + h_{\rm r,d} k_{\rm r} a_1 \tilde{n}_{\rm s,r}(m) \\ & + h_{\rm r,d} \left(\tilde{x}_{\rm s}^{\rm NL}(m) + \tilde{w}_{\rm r,d}(m) \right) + \tilde{n}_{\rm r,d}(m), \end{aligned} \tag{25}$$

where the third term is due to the nonlinearity of the relay PA. In the following subsections, first, by the use of the MRC method and considering the effects of the NLPA of the relay in (25), the suitable weights for combining $y_{\rm s,d}(m)$ and $y_{\rm r,d}(m)$ are derived. In addition, the symbols of the resulting distorted modulation constellation due to the PA nonlinearity are derived. Then, the feedforward compensation method is presented.

A. Modification of the MRC Coefficients with Considering the Nonlinear Effects of the PA

At the destination node, we use the MRC method for combining the received signals from the source and relay [41]. In order to achieve the maximum signal to interference and noise ratio (SINR) in this method, the coefficient of each branch has to be proportional to the root mean square of the transmitted signal power and complex conjugate of the respective channel coefficient, and also must be inversely proportional to the average power of noise and interference of that branch [3], [42]. First, we obtain the MRC coefficient related to the SD branch, i.e., k_1 in Fig. 2(a). The suitable coefficient for nominator of k_1 is $h_{\rm s,d}^* a_1^* \sqrt{P_{\rm s}} \mathcal{E}_g$, and since the power of the noise term at the output of the MF in (24) is $N_0 \mathcal{E}_g$ [31], we get

$$k_1 = \frac{h_{\rm s,d}^* a_1^* \sqrt{P_{\rm s}}}{N_0}. \tag{26}$$

Similarly, in order to obtain the proper MRC weight for the RD branch, with respect to $\tilde{y}_{\rm r,d}(m)$ in (25), the nominator should be $h_{\rm s,r}^* h_{\rm r,d}^* k_{\rm r} \left(a_1^*\right)^2 \sqrt{P_{\rm s}} \mathcal{E}_g$, and by taking into account

the impact of interference from the relay NLPA and destination noise on the denominator as the power $P_{\rm NI}$, we get

$$k_2^{MC} = \frac{h_{\rm s,r}^* h_{\rm r,d}^* k_{\rm r} \left(a_1^*\right)^2 \sqrt{P_{\rm s}} \mathcal{E}_g}{P_{\rm NI}}. \tag{27}$$

where $P_{\rm NI}$ is the power of noise and interference terms of $\tilde{y}_{\rm r,d}(m)$. The first term of $\tilde{y}_{\rm r,d}(m)$ is the linearly amplified information signal, and if we denote the summation of the other terms by $\hat{y}_{\rm r,d}(m)$, we can obtain

$$\begin{aligned} P_{\rm NI} &= {\rm E}\left\{\left|\hat{y}_{\rm r,d}(m)\right|^2\right\} \\ &= \int_{-\infty}^{+\infty}\int_{-\infty}^{+\infty} {\rm E}\left\{\hat{y}_{\rm r,d}(t_1)\hat{y}_{\rm r,d}(t_2)\right\} g(t_1)g(t_2)dt_1dt_2. \end{aligned} \tag{28}$$

In the sequel, we obtain $P_{\rm NI}$ for a third order NLPA ($N_p = 1$) by substituting (9) and (12) into (28) which yields

$$P_{\rm NI} = \int_{-\infty}^{+\infty}\int_{-\infty}^{+\infty} \left\{ \left|h_{\rm r,d}\right|^2 \sum_{m=2}^{8}\sum_{n=2}^{8} \beta_{mn} R_{2z_{\rm r}}^{(m,n)}(t,\tau) + R_{n_{\rm rd}}(\tau) \right\} g(t)g(\tau)dtd\tau. \tag{29}$$

Then, we substitute the correlation functions $R_{2z_{\rm r}}^{(m,n)}(t;\tau)$, obtained for (13), into (29), and by the use of (15) and (16) we transform them to the separate functions of t and τ. Finally, we have

$$P_{\rm NI} = \left|h_{\rm r,d}\right|^2 \sum_{m=2}^{8}\sum_{n=2}^{8} \beta_{mn} P^{(m,n)} + N_0 \mathcal{E}_g, \tag{30}$$

where for example, $P^{(7,7)}$ can be expressed as (31).

B. Estimation of Distorted Constellation

The suitable coefficients for SD and RD branches at destination in Fig. 2(a), i.e., k_1 and $k_1^{\rm MC}$, are computed in (26) and (27), and after combination we have

$$y_{\rm d}^{\rm MC}(m) = k_1 \tilde{y}_{\rm s,d}(m) + k_2^{\rm MC} \tilde{y}_{\rm r,d}(m). \tag{32}$$

The transmitted data symbol should be detected by the use of $y_{\rm d}^{\rm MC}(m)$. Note that the MF output signal of RD branch in (25) includes $\tilde{x}_{\rm s}^{\rm NL}(m)$ which denotes higher-order terms of the data symbols. These terms make the constellation diagram distorted and using the decision regions of the reference linear case for demodulation will result in increased probability of error. In order to deal with this nonlinear effect, we derive the distorted constellation in terms of the nonlinear model of the PA which can thereon be used in demodulation. First, we can rewrite $x_{\rm s}^{\rm NL}(t)$ in (7) as

$$\begin{aligned} x_{\rm s}^{\rm NL}(t) &= \sum_{i=1}^{N_p} a_{2i+1} k_{\rm r}^{2i+1} h_{\rm s,r} \left|h_{\rm s,r}\right|^{2i} a_1 \left|a_1\right|^{2i} P_{\rm s}^{\frac{(2i+1)}{2}} x_{\rm s}(t) \left|x_{\rm s}(t)\right|^{2i} \\ &= \sum_{i=1}^{N_p} a_{2i+1} k_{\rm r}^{2i+1} h_{\rm s,r} \left|h_{\rm s,r}\right|^{2i} a_1 \left|a_1\right|^{2i} P_{\rm s}^{\frac{(2i+1)}{2}} \\ &\quad \left\{ \sum_{m=-\infty}^{+\infty} s_{\rm m} \left|s_{\rm m}\right|^{2i} g^{(2i+1)}(t - mT) \right\} + x_{\rm s}^{\rm ISI}(t), \end{aligned} \tag{33}$$

where $x_{\rm s}^{\rm ISI}(t)$ includes the ISI terms. Then, the corresponding $\tilde{x}_{\rm s}^{\rm NL}(m)$ reads as follows

$$\begin{aligned} \tilde{x}_{\rm s}^{\rm NL}(m) = \sum_{i=1}^{N_p} a_{2i+1} k_{\rm r}^{2i+1} h_{\rm s,r} a_1 \left|h_{\rm s,r} a_1\right|^{2i} P_{\rm s}^{\frac{(2i+1)}{2}} \\ s_{\rm m} \left|s_{\rm m}\right|^{2i} \mathcal{E}_{g^{(i+1)}} + \tilde{x}_{\rm s}^{\rm ISI}(m), \end{aligned} \tag{34}$$

where $\mathcal{E}_{g^{(i+1)}}$ is the energy of $g^{(i+1)}(t)$. The mth sample at the output of RD branch can be obtained by substituting (34) into (25) which yields

$$\begin{aligned} \tilde{y}_{\rm r,d}(m) = \sum_{i=0}^{N_p} a_{2i+1} k_{\rm r}^{2i+1} h_{\rm s,r} h_{\rm r,d} a_1 \left|h_{\rm s,r} a_1\right|^{2i} P_{\rm s}^{\frac{(2i+1)}{2}} \\ s_{\rm m} \left|s_{\rm m}\right|^{2i} \mathcal{E}_{g^{(i+1)}} + h_{\rm r,d} k_{\rm r} a_1 \tilde{n}_{\rm s,r}(m) \\ + h_{\rm r,d} \left(\tilde{x}_{\rm s}^{\rm ISI}(m) + \tilde{w}_{\rm r,d}(m)\right) + \tilde{n}_{\rm r,d}(m), \end{aligned} \tag{35}$$

where the first part depends only on mth symbol and we can utilize it to modify the reference constellation points used in the detection. Therefore, using (24), (32), and (35), the centers of the distorted constellation points can be expressed as

$$\begin{aligned} s_n^{\rm MC} = s_n \Bigg(k_1 h_{\rm s,d} a_1 \sqrt{P_{\rm s}} \mathcal{E}_g + k_2^{\rm MC} \sum_{i=0}^{N_p} a_{2i+1} k_{\rm r}^{2i+1} h_{\rm s,r} h_{\rm r,d} a_1 \\ \left|h_{\rm s,r} a_1\right|^{2i} P_{\rm s}^{\frac{(2i+1)}{2}} \left|s_n\right|^{2i} \mathcal{E}_{g^{(i+1)}} \Bigg), \quad n \in \{1, ..., M\}, \end{aligned} \tag{36}$$

where M is the order of modulation, s_n is the nth symbol of the original constellation, and s_n^{MC} is the nth symbol of the modified reference constellation.

C. Feedforward Linearization at Destination Node

The correction of the output signal of the NLPA using another signal created at its input is called feedforward linearization [43]. In general, this method is applied to the transmitter by the use of the input data signal which is noiseless, however, in order to implement this method at the

$$\begin{aligned} P^{(7,7)} = N_0 \int_{-B}^{+B} \Bigg[\frac{\gamma_{\rm s,2,1}^2}{T^2} \sum_{m=-1}^{1}\sum_{n=-1}^{1} \rho_{\frac{m}{T}}^{(1,1)}(0) \rho_{\frac{n}{T}}^{(1,1)}(0) G\left(f - \frac{m}{T}\right) G\left(f + \frac{m}{T}\right) + \frac{\gamma_{\rm s,2,1}^2}{T^2} \sum_{m=-1}^{1}\sum_{n=-1}^{1} \left\{ G\left(f + \frac{m}{T}\right) G(f) \right\} \\ \star \left\{ G\left(f + \frac{n}{T}\right) G(f) \right\} \star \left\{ G\left(f - \frac{m+n}{T}\right) G(f) \right\} + \frac{\gamma_{\rm s,4,2}}{T} \sum_{m=-3}^{3} \left\{ G_2\left(f + \frac{m}{T}\right) G_2(f) \right\} \star \left\{ G\left(f - \frac{m}{T}\right) G(f) \right\} \Bigg] df. \end{aligned} \tag{31}$$

receiver a reference signal is needed [44]. In our system, from two received versions of data signal at the destination node, only the received signal from the relay contains nonlinear terms ($x_{\rm s}^{\rm NL}(t)$ in (10)). Hence, we argue that these nonlinear terms can be eliminated by the use of the received signal from the source. As shown in Fig. 2(b), we compensate the nonlinearity through a feedforward path from the SD branch to the RD branch. However, it should be noticed that the noise $n_{\rm s,d}(t)$ will also be amplified in this path.

In the feedforward path, first, $y_{\rm s,d}(t)$ is multiplied by $k_{\rm c}$ in order to make the coefficient of $x_{\rm s}(t)$ the same as the coefficient of that at the input of the NLPA at relay. This results in

$$k_{\rm c}=\frac{h_{\rm s,r}}{h_{\rm s,d}}k_{\rm r}. \tag{37}$$

Then from the resulting signal, according to the model of the NLPA at relay, the higher than first-order terms are regenerated and multiplied by $h_{\rm r,d}$ which yields $v_{\rm c}^{\rm FF}(t)$ as follows

$$\begin{aligned} v_{\rm c}^{\rm FF}(t) =&h_{\rm r,d}\sum_{i=1}^{N_p}a_{2{\rm i}+1}(k_c y_{\rm s,d}(t))\left|k_c y_{\rm s,d}(t)\right|^{2i}\\ =&h_{\rm r,d}\left(x_{\rm s}^{\rm NL}(t)+w_{\rm s,d}^{\rm FF}(t)\right), \end{aligned} \tag{38}$$

where $w_{\rm s,d}^{\rm FF}(t)$ includes the summation of multiplicative signal and noise terms. Now, the term $h_{\rm r,d}x_{\rm s}^{\rm NL}(t)$ which is regenerated at the output of the feedforward path can be used for the cancellation of the similar term in (10) in the RD branch. Hence, as can be seen in Fig. 2(b), the input signal of the MF in the RD branch through the use of (10) and (38) can be expressed as

$$\begin{aligned} y_{\rm r,d}^{\rm FF}(t) =&y_{\rm r,d}(t)-v_{\rm c}^{\rm FF}(t)\\ =&h_{\rm s,r}h_{\rm r,d}k_{\rm r}a_1^2\sqrt{P_s}x_s(t)+h_{\rm r,d}k_r a_1 n_{\rm s,r}(t)+n_{\rm r,d}(t)\\ &+h_{\rm r,d}\left(w_{\rm r,d}(t)-w_{\rm s,d}^{\rm FF}(t)\right). \end{aligned} \tag{39}$$

After sampling the MF output of the RD branch, the symbols $\tilde{y}_{\rm r,d}^{\rm FF}(m)$ are obtained. For the feedforward method, it is necessary to derive the MRC coefficient in the RD branch, which is here denoted by $k_2^{\rm FF}$. The numerator of $k_2^{\rm FF}$ is equal to that of $k_2^{\rm MC}$ in (27) and we have

$$k_2^{\rm FF}=\frac{h_{\rm s,r}^* h_{\rm r,d}^* k_{\rm r}\left(a_1^*\right)^2\sqrt{P_{\rm s}}\mathcal{E}_g}{P_{\rm NI}^{\rm FF}}, \tag{40}$$

where the power of the summation of the last four terms of $\tilde{y}_{\rm r,d}^{\rm FF}(m)$ related to the noise and interference is denoted by $P_{\rm NI}^{\rm FF}$. Note that, because $w_{\rm s,d}^{\rm FF}(t)$ contains $n_{\rm s,d}(t)$ it is uncorrelated with other noise and interference terms in (39). Thus, $P_{\rm NI}^{\rm FF}$ can be expressed as

$$P_{\rm NI}^{\rm FF}=P_{\rm NI}-P_{\rm s}^{\rm NL}+\left|h_{\rm r,d}\right|^2\left(P_{\tilde{w}_{\rm s,d}^{\rm FF}}-2\,{\rm Re}\{E_{\rm rs}\}\right), \tag{41}$$

where $P_{\rm NI}$ given in (28) is the power of noise and interference in the RD branch when there is no feedforward compensation, $P_{\rm s}^{\rm NL}$ is the power resulting from $\tilde{x}_{\rm s}^{\rm NL}(m)$ which is subtracted from $P_{\rm NI}$ because of the feedforward path, $P_{\tilde{w}_{\rm s,d}^{\rm FF}}$ is the power of $\tilde{w}_{\rm s,d}^{\rm FF}(m)$, ${\rm Re}\{\cdot\}$ stands for the real part of a complex number, and $E_{\rm rs}$ is equal to ${\rm E}\left\{\tilde{w}_{\rm r,d}^*(m)\tilde{w}_{\rm s,d}^{\rm FF}(m)\right\}$. Assuming the third order nonlinear model for the PA, $P_{\rm NI}$ is given by (30). Also, $P_{\rm s}^{\rm NL}$ includes non-zero terms of $P_{\rm NI}$ which are related to $\tilde{x}_{\rm s}^{\rm NL}(m)$ as follows

$$P_{\rm s}^{\rm NL}=\left|h_{\rm r,d}\right|^2\left(\beta_{33}P^{(3,3)}+2\,{\rm Re}\{\beta_{38}\}P^{(3,8)}\right). \tag{42}$$

In order to derive $P_{\tilde{w}_{\rm s,d}^{\rm FF}}$, first we write $w_{\rm s,d}^{\rm FF}(t)$ using (8) and (38) as

$$\begin{aligned} w_{\rm s,d}^{\rm FF}(t)=a_3k_r^3\Bigg\{&\frac{h_{\rm s,r}}{h_{\rm s,d}^2}\left|h_{\rm s,r}\right|^2\sqrt{P_{\rm s}}a_1^*x_s^*(t)n_{\rm s,d}^2(t)\\ &+2\frac{h_{\rm s,r}}{h_{\rm s,d}}\left|h_{\rm s,r}\right|^2\left|a_1\right|^2P_{\rm s}\left|x_s(t)\right|^2n_{\rm s,d}(t)+\frac{h_{\rm s,r}}{h_{\rm s,d}^*}\left|h_{\rm s,r}\right|^2a_1^2\\ &P_{\rm s}x_s^2(t)n_{\rm s,d}^*(t)+\frac{h_{\rm s,r}\left|h_{\rm s,r}\right|^2}{h_{\rm s,d}\left|h_{\rm s,d}\right|^2}n_{\rm s,d}(t)\left|n_{\rm s,d}(t)\right|^2\\ &+2\frac{h_{\rm s,r}\left|h_{\rm s,r}\right|^2}{\left|h_{\rm s,d}\right|^2}a_1\sqrt{P_{\rm s}}x_s(t)\left|n_{\rm s,d}(t)\right|^2\Bigg\}. \end{aligned} \tag{43}$$

As a result of the moment theorem stated in Appendix A, the cross-correlation of all terms of $w_{\rm s,d}^{\rm FF}(t)$ are zero. Hence, using the same derivation as in Section IV-A we get

$$\begin{aligned} P_{\tilde{w}_{\rm s,d}^{\rm FF}}=\left|a_3\right|^2k_r^6\Bigg\{&\frac{\left|h_{\rm s,r}\right|^6}{\left|h_{\rm s,d}\right|^4}\left|a_1\right|^2P_{\rm s}\left(P^{(5,5)}+4P^{(8,8)}\right)\\ &+\frac{\left|h_{\rm s,r}\right|^6}{\left|h_{\rm s,d}\right|^6}P^{(6,6)}+\frac{\left|h_{\rm s,r}\right|^6}{\left|h_{\rm s,d}\right|^2}\left|a_1\right|^4P_{\rm s}^2\left(P^{(4,4)}+4P^{(7,7)}\right)\Bigg\}. \end{aligned} \tag{44}$$

and we have

$$E_{\rm rs}=4\left|a_1\right|^2\left|a_3\right|^2k_r^6\frac{\left|h_{\rm s,r}\right|^4}{\left|h_{\rm s,d}\right|^2}P_{\rm s}P^{(1,1)}\left(2N_0B\right)^2. \tag{45}$$

We observe from $P_{\rm NI}^{\rm FF}$ in (41) that the feedforward path causes the power of noise and interference in the RD branch, i.e., $P_{\rm NI}$, decreases by $P_{\rm s}^{\rm NL}$, however, third and fourth terms of $P_{\rm NI}^{\rm FF}$ may cause it to become greater than $P_{\rm NI}$. Therefore, in order that the feedforward compensation does not lead to the increase of the power of noise and interference, it must be active only when the following condition holds

$$P_{\rm NI}^{\rm FF}<P_{\rm NI}, \tag{46}$$

and when the feedforward compensation is not active, the method of the previous section can be used instead.

V. Analytical BER

In this section, we derive the error probabilities of the suggested compensation methods. To obtain the average BER, first, we calculate the symbol error rate (SER) for a given fading state under block fading assumption as follows [31]

$$Pr_{\rm SER}=\sum_{i=1}^{M}P(s_i)\sum_{j\in D_i}Q\left(\sqrt{\frac{d_{ij}^2}{2P_{\rm ni}}}\right), \tag{47}$$

where $P(s_i)$ is the prior probability that data symbol s_i is transmitted, D_i is the number of subregions for the ith data symbol, $P_{\rm ni}$ is the power of noise and interference of the received data symbols after combination of two branches, and

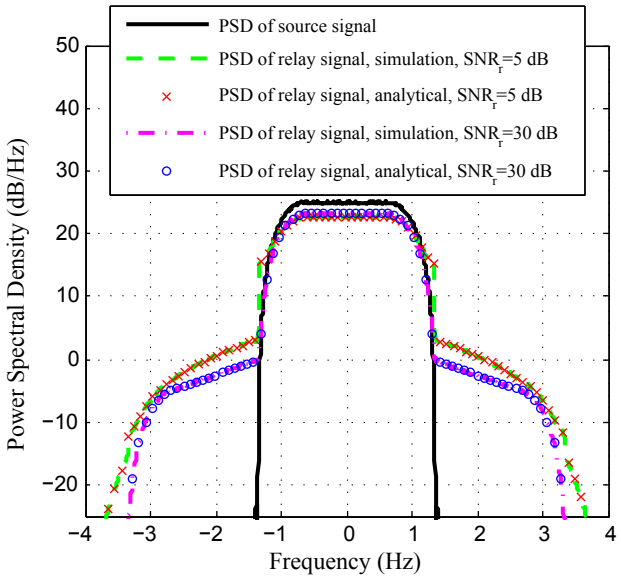

Fig. 3. The PSD of the source output signal for $P_{\rm s} = 2$ dB, and the PSD of the relay output signal for $P_{\rm r} = 2$ dB and two different $\text{SNR}_{\rm r}$s.

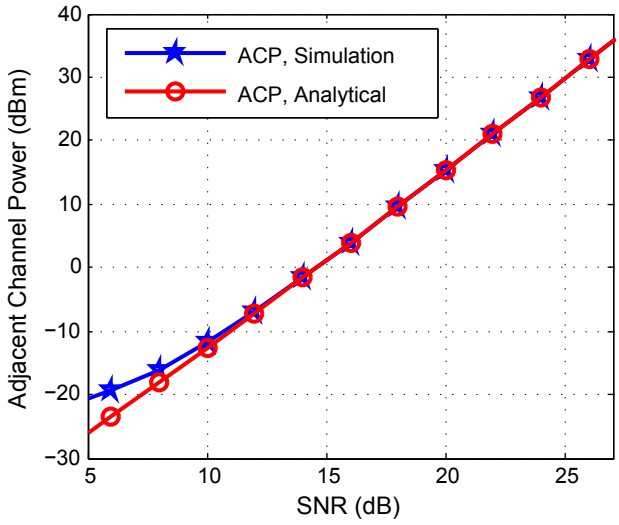

Fig. 4. The ACP of the output signal of NLPA at the relay node in terms of transmit SNR.

d_{ij} is the Euclidean distance between ith and jth adjacent data symbols in the constellation as $d_{ij} = \|s_i - s_j\|$. An example distorted 16-QAM constellation and the corresponding decision regions are presented in Fig. 2 of [12].

For the method of modified reference constellation and MRC weights, the data symbols of the distorted constellation is derived as (36). In this method, from (24) and (32), $P_{\rm ni}$ is given by

$$P_{\rm ni} = |k_1|^2 N_0 \mathcal{E}_g + \left|k_2^{\rm MC}\right|^2 P_{\rm ni,rd}^{\rm MC}, \tag{48}$$

where for a third order NLPA we have

$$P_{\rm ni,rd}^{\rm MC} = |h_{\rm r,d}|^2 \left(P_{\rm ISI} + \sum_{\substack{m=2 \\ m\neq 3}}^{8} \sum_{\substack{n=2 \\ n\neq 3}}^{8} \beta_{mn} P^{(m,n)} \right) + N_0 \mathcal{E}_g, \tag{49}$$

and $P_{\rm ISI}$ is the average power of $\tilde{x}_{\rm s}^{\rm ISI}(m)$ which includes the ISI terms after the MF of rd branch. The calculation of $P_{\rm ISI}$ is presented in Appendix C.

Similarly, in the feedforward method, $P_{\rm ni}$ can be computed as

$$P_{\rm ni} = |k_1|^2 N_0 \mathcal{E}_g + \left|k_2^{\rm FF}\right|^2 P_{\rm NI}^{\rm FF}, \tag{50}$$

where $P_{\rm NI}^{\rm FF}$ is given in (41). In this method, since the feedforward path from sd to rd branch removes the higher-order terms of the information signal (Fig. 2(b)), the constellation points after the combination are

$$s_m^{\rm FF} = s_m \left(k_1 h_{\rm s,d} a_1 \sqrt{P_{\rm s}} \mathcal{E}_g + k_2^{\rm FF} a_1^2 k_{\rm r} h_{\rm s,r} h_{\rm r,d} \sqrt{P_{\rm s}} \mathcal{E}_g \right), \quad m \in \{1, ..., M\}. \tag{51}$$

It is worth mentioning that the average SER can be obtained by averaging $Pr_{\rm SER}$ over all fading channels [40] as

$$Pr_{\rm SER}^{\rm avg} = \mathrm{E}_{h_{\rm s,r}, h_{\rm r,d}, h_{\rm s,d}} \{Pr_{\rm SER}\} \tag{52}$$

$$= \int_{h_{\rm s,r}} \int_{h_{\rm r,d}} \int_{h_{\rm s,d}} Pr_{\rm SER} f_{h_{\rm s,r}}(u) f_{h_{\rm r,d}}(v) f_{h_{\rm s,d}}(z) du dv dz, \tag{53}$$

where $f_{h_{\rm s,r}}(u)$, $f_{h_{\rm r,d}}(v)$, and $f_{h_{\rm s,d}}(z)$ are the probability density functions of $h_{\rm s,r}$, $h_{\rm r,d}$, and $h_{\rm s,d}$, respectively. The expectation in (52) can be calculated by the Monte Carlo method [45]. In addition, by the use of Gray encoding, the equivalent average BER is given by the average SER divided by $log_2(M)$ [31].

VI. Numerical Results

In this section, the performance of the cooperative CR system with the NLPA at the relay node, and the performance improvement due to the proposed nonlinearity compensation methods are evaluated using the numerical and simulation results. The modulation scheme is 16-QAM, the normalized symbol time duration is 0.5, and the pulse shape is root raised cosine (RRC) with a roll off factor 0.35 which results in a normalized bandwidth of $B = 1.35$ [40]. The coefficient of the linear PA at the source node is set as $a_1 = 14$, and the NLPA at the relay node has the coefficients a_1 and a_3 where $a_3 = -0.6\mathrm{e}^{(j\pi/10)}$. Please note that, as can be seen later, the values of a_1 and a_3 are selected such that the BER of the receiver node be better than 10^{-3}. We assume that $P_{\rm r} = P_{\rm s}$, the fading channel coefficients are zero-mean complex Gaussian distributed with unit variance, and the normalized noise density reads $N_0 = 1$.

Fig. 3 shows the spectral regrowth of the output signal of the relay node due to its PA nonlinearity compared to the PSD of the output signal of the source node in terms of $\text{SNR}_{\rm r}$ which is defined in (21). The PSD of the relay output signal is illustrated for two cases including $\text{SNR}_{\rm r} = 5$ dB

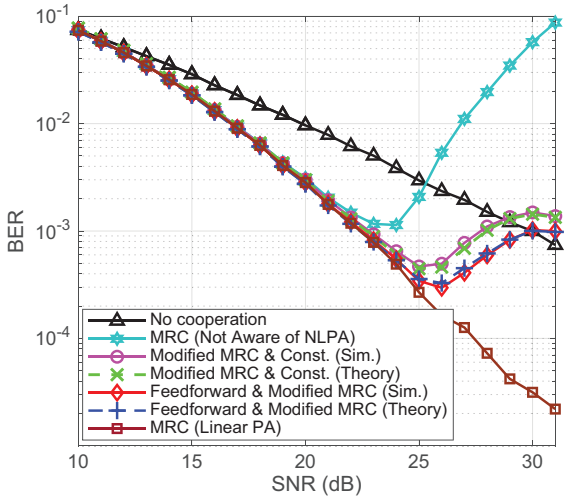

Fig. 5. Average BER performance versus transmit SNR.

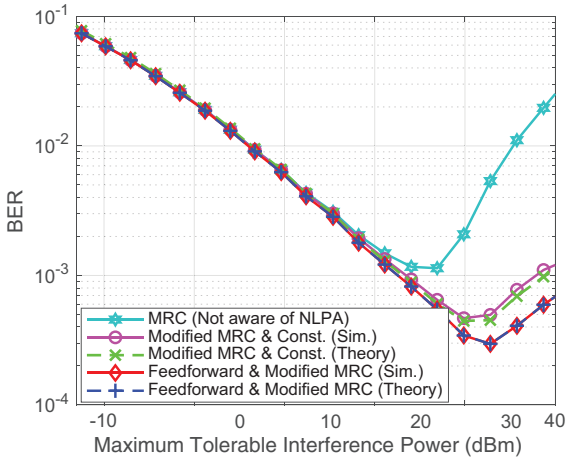

Fig. 6. Achievable BER versus interference power constraint of the PU.

(dashed curves) and $\mathrm{SNR_r} = 30$ dB (dashed-dotted curves) when $P_\mathrm{s} = P_\mathrm{r} = 2$ dB. The analytical PSDs demonstrate an excellent agreement with the Monte Carlo simulated ones. Change of $\mathrm{SNR_r}$ when P_s and P_r are fixed is due to the variation of fading channel gain between source and relay nodes, i.e., $|h_{\mathrm{s,r}}|^2$, and hence, as can be seen, PSD of the output signal of relay with NLPA, changes in different fading blocks. When P_s and P_r are fixed, and $\mathrm{SNR_r}$ is smaller, more spectral regrowth is observed. This is because at the input of the NLPA, the PSD of the noise-free data signal is more concentrated in the center of the bandwidth, while the noise PSD is constant, and hence, the PSD of the summation of noise and data signal at the output of the NLPA is more spread when the noise power is higher.

We assume the adjacent channel of the relay band in frequency domain is from B to 3B, and define transmit SNR as $\mathrm{SNR} \triangleq |a_1|^2 P_\mathrm{s} \mathcal{E}_g / N_0$. In Fig. 4, with Monte Carlo simulation, the ACP is obtained in terms of transmit SNR. In addition, using (22), the curve of analytical PSD is also plotted where it matches well with the simulation results. This figure is very useful in determining the interference power from the relay to the PUs of adjacent channels in the CR network context.

Fig. 5 illustrates the BER performance of a conventional MRC receiver and the proposed techniques in terms of transmit SNR. It is assumed that the conventional MRC is not aware of nonlinearity. The curves related to two cases where there is no cooperation (direct transmission) and where the relay has linear PA ($a_3 = 0$) are also illustrated which can be considered respectively as the upper and lower bounds for the other curves. For a fair comparison, the power of source is doubled in no cooperation case. The analytical BER curves obtained by the use of Section V match well with simulations which validates the analysis. To compute the expected value in (52) by the Monte Carlo method for each SNR, the fading channel coefficients needed for 5000 fading blocks are generated with complex Gaussian distribution; Next, in each fading block, the analytical equation (47) for Pr_{SER} is calculated, and then, 5000 samples of Pr_{SER} are averaged. As can be seen in Fig. 5, when the conventional MRC is not aware of the nonlinear behavior of PA at the relay, it cannot achieve BER better than 10^{-3}, but the modified MRC technique, and the modified MRC and reference constellation based one have clearly better performance than it at larger transmit SNR values. However, the feedforward technique shows better BER performance than the other one and achieves a BER of 3×10^{-4}. Note that the reason for upward movement of the curves after the bending points is that the nonlinear interference power overtakes the information signal power, and hence, decreases the SINR which leads to the increase of BER.

In Fig. 6, the achievable BER is investigated with respect to the maximum tolerable interference power at the PU of the adjacent channel. In order to get this result, we assume that the PU is active at the adjacent channel of the band of our cooperative system, and the average channel gain between the relay node and the PU in that adjacent channel is one. Therefore, the average ACI to the PU in terms of SNR of the cooperative system is equal to the ACP presented in Fig. 4. The ACI must meet the given interference power constraint of the PU, and hence, this constraint restricts the transmit power of the cooperative system. On the other hand, restriction of the transmit power leads to the limitation of the destination SNR, and consequently, BER restriction. Fig. 6 shows the effect of the maximum tolerable interference power of the PU, i.e., Q, on the BER performance of cooperative cognitive radio system. As can be seen, the theoretical BER curves are in excellent agreement with the simulation results, and the feedforward technique outperforms the other one.

VII. Conclusion

Analysis of noise and interference in a cooperative CR network with AF protocol under an NLPA at the relay has been presented in this paper. Furthermore, two alternative methods to reduce the effects of relay NLPA at the destination receiver were proposed. Although we consider the transmission band of the cooperative system to be a spectrum hole, the spectral

regrowth due to the relay NLPA causes interference to the PUs which use the adjacent bands. For the computation of such interference, we derived the PSD of the relay NLPA output signal when the data signal is digitally modulated and has a band-limited pulse shape. After that, for the MRC receiver with MF in each branch of the destination node, we derived the distorted modulation constellation, which can be used as the reference constellation in the symbol detection at the destination receiver. As an alternative enhancement method at the destination receiver, a so-called feedforward technique was also proposed, which uses the direct received signal from the source node to suppress the higher-order nonlinear distortion terms due to the relay NLPA. For both proposed methods, we derived the appropriate MRC coefficients and theoretical BER expressions with respect to the noise and nonlinear interference powers. We evaluated the analytical PSD and ACP numerically, and verified them through simulation results, evidencing a very good match between the analytical and simulation results. Furthermore, the numerical results demonstrated the effect of the source-relay channel gain on the output PSD of the NLPA at the relay when the input power to the NLPA was fixed. Finally, we studied the achievable end-to-end average BER performance of the proposed techniques in terms of transmit SNR as well as the maximum tolerable interference power of the PU by theory and simulation. Noticeable improvement was achieved through the proposed methods in comparison to the case where the destination was not aware of the nonlinear behavior of the NLPA. Moreover, simulation results closely match the analysis. As future works, the performance of this system model can be analyzed in terms of capacity and outage probability. Also, more relays with NLPAs in a two or multi-hop wireless network can be considered when their ACIs to the PUs must be limited, and an optimal path in each block fading can be found.

APPENDIX A
A MOMENT THEOREM

In general, for the zero-mean complex Gaussian process $n(t)$, if $i \neq j$ we have the following moment theorem [35]

$$\mathrm{E}\left\{n(t_{m_1})n(t_{m_2})\dots n(t_{m_i})n^*(t_{l_1})n^*(t_{l_2})\dots n^*(t_{l_j})\right\} = 0, \tag{54}$$

where m_k and l_k are integer numbers.

APPENDIX B
DERIVATION OF $R_{2z_\mathrm{r}}^{(7,7)}(t;\tau)$

In this section, the autocorrelation function $R_{2z_\mathrm{r}}^{(7,7)}(t;\tau)$ which is given in (14) is derived. By the use of (12) and (13) we have

$$R_{2z_\mathrm{r}}^{(7,7)}(t;\tau)=\mathrm{E}\left\{|x_\mathrm{s}(t)|^2\,|x_\mathrm{s}(t+\tau)|^2\right\}\mathrm{E}\left\{n_{\mathrm{s,r}}(t)n_{\mathrm{s,r}}^*(t+\tau)\right\}, \tag{55}$$

where the second expectation is equal to $R_{n_{\mathrm{s,r}}}(\tau)$. Because the expected values of $x_\mathrm{s}(t)$ and $x_\mathrm{s}^*(t)\,|x_\mathrm{s}(t+\tau)|^2$ are zero, $\mathrm{E}\left\{|x_\mathrm{s}(t)|^2\,|x_\mathrm{s}(t+\tau)|^2\right\}$ is equal to $\mathrm{cov}\left\{x_\mathrm{s}(t), x_\mathrm{s}(t)\,|x_\mathrm{s}(t+\tau)|^2\right\}$, and hence, equals $\mathrm{cum}\left\{x_\mathrm{s}(t), x_\mathrm{s}^*(t)\,|x_\mathrm{s}(t+\tau)|^2\right\}$ where $\mathrm{cov}\{\cdot\}$ denotes the covariance. In order to expand this cumulant of products of $x_\mathrm{s}(t)$ in terms of joint cumulants, we utilize Leonov-Shiryaev formula [37], [38]. To do so, first, we write the individual elements of the first argument of $\mathrm{cum}\left\{x_\mathrm{s}(t), x_\mathrm{s}^*(t)\,|x_\mathrm{s}(t+\tau)|^2\right\}$ in the first row of the following two-way table, and list the individual elements of the second argument of the cumulant in the second row as

$x_\mathrm{s}(t)$		
$x_\mathrm{s}^*(t)$	$x_\mathrm{s}(t+\tau)$	$x_\mathrm{s}^*(t+\tau)$

Then from this table, we write the indecomposable partitions defined in [37, p. 20] as follows

$$\begin{aligned}&[\{x_\mathrm{s}(t), x_\mathrm{s}^*(t)\}, \{x_\mathrm{s}(t+\tau), x_\mathrm{s}^*(t+\tau)\}]\\ &[\{x_\mathrm{s}(t), x_\mathrm{s}^*(t+\tau)\}, \{x_\mathrm{s}^*(t), x_\mathrm{s}(t+\tau)\}]\\ &[\{x_\mathrm{s}(t), x_\mathrm{s}^*(t), x_\mathrm{s}(t+\tau), x_\mathrm{s}^*(t+\tau)\}]\end{aligned}$$

Now, in order to derive $\mathrm{E}\left\{|x_\mathrm{s}(t)|^2\,|x_\mathrm{s}(t+\tau)|^2\right\}$, we obtain the multiplication of the cumulants of the subsets in each partition, and then, add the results together as follows

$$\begin{aligned}&\mathrm{cum}\{x_\mathrm{s}(t), x_\mathrm{s}^*(t)\}\,\mathrm{cum}\{x_\mathrm{s}(t+\tau), x_\mathrm{s}^*(t+\tau)\}\\ &+\mathrm{cum}\{x_\mathrm{s}(t), x_\mathrm{s}^*(t+\tau)\}\,\mathrm{cum}\{x_\mathrm{s}^*(t), x_\mathrm{s}(t+\tau)\}\\ &+\mathrm{cum}\{x_\mathrm{s}(t), x_\mathrm{s}^*(t+\tau), x_\mathrm{s}(t+\tau), x_\mathrm{s}^*(t+\tau)\}\\ &=C_{2\mathrm{x}}(t;0^*)C_{2\mathrm{x}}(t+\tau;0^*)+C_{2\mathrm{x}}(t;\tau^*)C_{2\mathrm{x}}(t^*;\tau)\\ &\quad+C_{4\mathrm{x}}(t;0^*,\tau,\tau^*).\end{aligned} \tag{56}$$

Because $C_{2x_\mathrm{s}}(t;\tau^*)$ is the conjugate of $C_{2x_\mathrm{s}}(t^*;\tau)$, we obtain the desired result in (14).

APPENDIX C
DERIVATION OF P_{ISI}

In this appendix, we obtain the average power of $\tilde{x}_\mathrm{s}^{\mathrm{ISI}}(m)$ in (34) for an NLPA with third order of nonlinearity ($N_p = 1$) as follows

$$P_{\mathrm{ISI}} = \mathrm{E}\left\{\left|\tilde{x}_\mathrm{s}^{\mathrm{ISI}}(m)\right|^2\right\}, \tag{57}$$

where $\tilde{x}_\mathrm{s}^{\mathrm{ISI}}(m)$ is given by

$$\begin{aligned}\tilde{x}_\mathrm{s}^{\mathrm{ISI}}(m) &= a_3 k_\mathrm{r}^3 h_{\mathrm{s,r}} a_1\,|h_{\mathrm{s,r}}a_1|^2\,P_\mathrm{s}^{\frac{3}{2}}\\ &\left\{\int_{-\infty}^{+\infty} x_s^*(t)x_s^2(t)g(t-mT)dt - s_\mathrm{m}\,|s_\mathrm{m}|^2\,\mathcal{E}_{g^{(2)}}\right\}.\end{aligned} \tag{58}$$

Substituting (1) into (58) yields

$$\tilde{x}_{\mathrm{s}}^{\mathrm{ISI}}(m) = a_3 k_{\mathrm{r}}^3 h_{\mathrm{s,r}} a_1 \left|h_{\mathrm{s,r}} a_1\right|^2 P_{\mathrm{s}}^{\frac{3}{2}} \Bigg\{ \sum_{n=-\infty}^{+\infty} \sum_{n'=-\infty}^{+\infty} s_n^* s_{n'}^2 \underbrace{\int_{-\infty}^{+\infty} g(t-nT) g^2(t-n'T) g(t-mT) dt}_{\triangleq F_{n,n',m}} + \sum_{n=-\infty}^{+\infty} \sum_{\substack{n_1',n_2'=-\infty \\ n_1' \neq n_2'}}^{+\infty} s_n^* s_{n_1'} s_{n_2'} \int_{-\infty}^{+\infty} g(t-nT) g(t-n_1'T) g(t-n_2'T) g(t-mT) dt - s_{\mathrm{m}} \left|s_{\mathrm{m}}\right|^2 \mathcal{E}_{g^{(2)}} \Bigg\}. \quad (59)$$

Note that because the pulse shape $g(t)$ decreases with increasing t, we can simplify (59). As an example, for the RRC pulse shape with roll-off factor 0.35, $F_{n,n',m} \simeq 0$ for $|m-n| > 2$ or $|m-n'| > 2$. Substituting (59) into (57) and using the moment properties of the data symbols s_m according to the given modulation type, we obtain P_{ISI}.

REFERENCES

[1] A. Nosratinia, T. E. Hunter, and A. Hedayat, "Cooperative communication in wireless networks," *IEEE Commun. Mag.*, vol. 42, no. 10, pp. 74–80, Oct. 2004.

[2] J. Qi, S. Aissa, and M.-S. Alouini, "Performance analysis of AF cooperative systems with HPA nonlinearity in semi-blind relays," in *Proc. IEEE Global Commun. Conf. (Globecom)*, California, USA, 2012.

[3] K. J. R. Liu, A. K. Sadek, W. Su, and A. Kwasinski, *Cooperative Communications and Networking*. New York: Cambridge Univ. Press, 2009.

[4] C. Zhang, Q. Du, Y. Wang, and G. Wei, "Optimal relay power allocation for amplify-and-forward OFDM relay networks with deliberate clipping," in *Proc. IEEE Wireless Commun. Netw. Conf. (WCNC)*, Paris, France, Apr. 2012, pp. 381–386.

[5] J. N. Laneman, D. N. C. Tse, and G. W. Wornel, "Cooperative diversity in wireless networks: Efficient protocols and outage behavior," *IEEE Trans. Inform. Theory*, vol. 50, no. 12, pp. 3062–3080, Dec. 2004.

[6] P. A. Anghel and M. Kaveh, "Exact symbol error probability of a cooperative network in a Rayleigh-fading environment," *IEEE Trans. Wireless Commun.*, vol. 3, no. 5, p. 14161421, Sep. 2004.

[7] G. Gur and F. Alagoz, "Green wireless communications via cognitive dimension: An overview," *IEEE Netw.*, vol. 25, no. 2, pp. 50–56, Mar./Apr. 2011.

[8] A. Mohammadi and F. M. Ghannouchi, *RF Transceiver Design for MIMO Wireless Communications*. Springer, 2012.

[9] S. C. Cripps, *RF Power Amplifiers for Wireless Communications*, 2nd ed. Norwood, MA: Artech House, 2006.

[10] P. M. Lavradore, T. R. Cunha, P. M. Cabral, and J. C. Pedro, "The linearity-efficiency compromise," *IEEE Microw. Mag.*, vol. 11, no. 5, pp. 44–58, Aug. 2010.

[11] J. Qi and S. Aissa, "Analysis and compensation of power amplifier nonlinearity in MIMO transmit diversity systems," *IEEE Trans. Veh. Technol.*, vol. 59, no. 6, pp. 2921–2931, Jul. 2010.

[12] ——, "On the power amplifier nonlinearity in MIMO transmit beamforming systems," *IEEE Trans. Commun.*, vol. 60, no. 3, pp. 876–887, Mar. 2012.

[13] P. K. Singya, N. Kumar, and V. Bhatia, "Mitigating NLD for wireless networks," *IEEE Microw. Mag.*, vol. 18, no. 5, pp. 73–90, Jun. 2017.

[14] A. Goldsmith, S. Jafar, I. Maric, and S. Srinivasa, "Breaking spectrum gridlock with cognitive radios: An information theoretic perspective," *Proc. IEEE*, vol. 97, no. 5, pp. 894–914, May 2009.

[15] M. Majidi, A. Mohammadi, and A. Abdipour, "Analysis of the power amplifier nonlinearity on the power allocation in cognitive radio networks," *IEEE Tran. Commun.*, vol. 62, no. 2, pp. 467–477, Feb. 2014.

[16] M. Baghani, A. Mohammadi, M. Majidi, and M. Valkama, "Uplink resource allocation in multiuser multicarrier cognitive radio networks under power amplifier nonlinearity," *Trans. Emerg. Telecommun. Technol.*, vol. 28, no. 10, Mar. 2017.

[17] Q. Zhang, J. Jia, and J. Zhang, "Cooperative relay to improve diversity in cognitive radio networks," *IEEE Commun. Mag.*, vol. 47, no. 2, pp. 111–117, Feb. 2009.

[18] K. B. Letaief and W. Zhang, "Cooperative communications for cognitive radio networks," *Proc. IEEE*, vol. 97, no. 5, pp. 878–893, May 2009.

[19] M. Naeem, A. Anpalagan, M. Jaseemuddin, and D. C. Lee, "Resource allocation techniques in cooperative cognitive radio networks," *IEEE Commun. Surv. Tutor.*, vol. 16, no. 2, pp. 729–744, Nov. 2013.

[20] T. Q. Duong, D. B. da Costa, M. Elkashlan, and V. N. Q. Bao, "Cognitive amplify-and-forward relay networks over Nakagami-m fading," *IEEE Trans. Veh. Technol.*, vol. 61, no. 5, pp. 2368–2374, Jun. 2012.

[21] M. Xia and S. Aissa, "Underlay cooperative AF relaying in cellular networks: performance and challenges," *IEEE Commun. Mag.*, vol. 51, no. 12, pp. 170–176, Dec. 2013.

[22] M. Baghani, A. Mohammadi, M. Majidi, and M. Valkama, "Analysis and rate optimization of OFDM-based cognitive radio networks under power amplifier nonlinearity," *IEEE Trans. Commun.*, vol. 62, no. 10, pp. 3410–3419, Oct. 2014.

[23] D. Dardari, V. Tralli, and A. Vaccari, "A theoretical characterization of nonlinear distortion effects in OFDM systems," *IEEE Trans. Commun.*, vol. 48, no. 10, pp. 1755–1764, Oct. 2000.

[24] C. A. R. Fernandes, D. B. da Costa, and A. L. F. de Almeida, "Performance analysis of cooperative amplify-and-forward orthogonal frequency division multiplexing systems with power amplifier nonlinearity," *IET Commun.*, vol. 8, no. 18, pp. 3223–3233, Dec. 2014.

[25] N. Kumar, S. Sharma, and V. Bhaita, "Performance analysis of OFDM-based nonlinear AF multiple-relay systems," *IEEE Wireless Commun. Lett.*, vol. 6, no. 1, pp. 122–125, Feb. 2017.

[26] N. Kumar, P. K. Singya, and V. Bhatia, "Performance analysis of orthogonal frequency division multiplexing-based cooperative amplify-and-forward networks with non-linear power amplifier over independently but not necessarily identically distributed Nakagami-m fading channels," *IET Commun.*, vol. 11, no. 7, pp. 1008–1020, May 2017.

[27] E. Balti and M. Guizani, "Impact of non-linear high-power amplifiers on cooperative relaying systems," *IEEE Trans. Commun.*, vol. 65, no. 10, pp. 4163 – 4175, Oct. 2017.

[28] S. R. C. Magalhaes, C. A. R. Fernandes, and L. C. S. Teles, "Relay selection methods for cooperative OFDM systems with nonlinear power amplifiers," in *Proc. IEEE Symp. Comput. Commun. (ISCC)*, Brazil, 2018, pp. 990–995.

[29] V. D. Razo, T. Riihonen, F. Gregorio, S. Werner, and R. Wichman, "Nonlinear amplifier distortion in cooperative amplify-and-forward OFDM systems," in *Proc. IEEE Wireless Commun. Netw. Conf. (WCNC)*, Hungary, 2009, pp. 352–356.

[30] Q. Liu, W. Zhang, X. Ma, and G. T. Zhou, "Designing peak power constrained amplify-and-forward relay networks with cooperative diversity," *IEEE Trans. Wireless Commun.*, vol. 11, no. 5, pp. 1733–1743, May 2012.

[31] J. G. Proakis and M. Salehi, *Digital Communications*, 5th ed. New York: MacGraw-Hill, 2008.

[32] S. Benedetto and E. Biglieri, *Principles of Digital Transmission with Wireless Applications*. New York, NY, USA: Kluwer Academic/Plenum Publishers, 1999.

[33] G. T. Zhou, "Analysis of spectral regrowth of weakly nonlinear power amplifiers," *IEEE Commun. Lett.*, vol. 4, no. 11, pp. 357–359, Nov. 2000.

[34] R. Raich and G. T. Zhou, "Spectral analysis for bandpass nonlinearity with cyclostationary input," in *Proc. IEEE Int. Conf. Acoust., Speech, Signal Process. (ICASSP)*, Quebec, Canada, 2004, pp. ii465–ii468.

[35] I. S. Reed, "On a moment theorem for complex Gaussian processes," *IRE Trans. Inform. Theory*, vol. 8, no. 3, pp. 194–195, Apr. 1962.

[36] O. A. Dobre, Y. Bar-Ness, and W. Su, "Higher-order cyclic cumulants for high order modulation classification," in *Proc. IEEE Mil. Commun. Conf. (MILCOM)*, vol. 1, Boston, MA, USA, Oct. 2003, pp. 112–117.

[37] D. R. Brillinger, *Time Series: Data Analysis and Theory*. San Francisco, CA: Holden-day Inc., 1981.

[38] R. Raich, "Nonlinear system identification and analysis with applications to power amplifier modeling and power amplifier predistortion," Ph.D. dissertation, School of Electrical and Computer Engineering, Georgia Institute of Technology, Mar. 2004.

[39] M. Majidi, A. Mohammadi, and A. Abdipour, "Accurate analysis of spectral regrowth of nonlinear power amplifier driven by cyclostationary

modulated signals," *Springer J. Analog Integr. Circuits Signal Process.*, vol. 74, no. 2, pp. 425–437, Feb. 2013.
[40] A. Goldsmith, *Wireless Communications*. Cambridge University Press, 2005.
[41] J. N. Laneman and G. W. Wornell, "Energy-efficient antenna sharing and relaying for wireless networks," in *Proc. IEEE Wireless Commun. Netw. Conf. (WCNC)*, vol. 1, Chicago, IL, USA, 2000, pp. 7–12.
[42] D. G. Brennan, "Linear diversity combining techniques," *Proc. IEEE*, vol. 91, no. 2, pp. 331–356, Feb. 2003.
[43] A. Gokceoglu, A. Ghadam, and M. Valkama, "Steady-state performance analysis and step-size selection for LMS-adaptive wideband feedforward power amplifier linearizer," *IEEE Trans. Signal Process.*, vol. 60, no. 1, pp. 82–99, Jan. 2012.
[44] M. Grimm, M. Allen, J. Marttila, M. Valkama, and R. Thoma, "Joint mitigation of nonlinear RF and baseband distortions in wideband direct-conversion receivers," *IEEE Trans. Microw. Theory Techn.*, vol. 62, no. 1, pp. 166–182, Jan. 2014.
[45] R. Y. Rubinstein and D. P. Kroese, *Simulation and the Monte Carlo Method*, 3rd ed. New Jersey: Wiley, 2017.

Mahdi Majidi (S'07-M'14) received the B.Sc. degree in electrical engineering from Isfahan University of Technology, Isfahan, Iran, in 2004, and the M.S. and Ph.D. degrees in electrical engineering from Amirkabir University of Technology (Tehran Polytechnic), Tehran, Iran, in 2007 and 2014, respectively. In 2012, he joined the Communications and Networks Laboratory, Department of Electrical and Computer Engineering, National University of Singapore (NUS), Singapore, as a Visiting Ph.D. Student. In 2015, he worked as a researcher at the Iran Telecommunication Research Center (ITRC). Since 2016, he is an assistant professor of the Department of Electrical and Computer Engineering, University of Kashan, Iran. His research interests include numerical and analytical optimization methods, wireless transceiver design, wireless powered communications, cognitive radio networks, cooperative and MIMO communications.

Abbas Mohammadi (S'88-M'00-SM'08) received his B.Sc. degree in Electrical Engineering from Tehran University, Iran in 1988, and his M.Sc. and Ph.D. degrees in Electrical Engineering from the University of Saskatchewan, Canada, in 1995 and 1999, respectively. In 1998, he joined Vecima Networks Inc., Victoria, Canada, as a senior research engineer where he conducted research on Wireless Communications. Since March 2000, he has been with the Electrical Engineering Department of Amirkabir University of Technology (Tehran Polytechnic), Tehran, Iran, where he is currently a professor. He is a senior member of IEEE. Dr. Mohammadi has been an ICORE visiting professor in Electrical and Computer Engineering Department of the University of Calgary, Canada, and Nokia visiting professor in Tampere University of Technology, Finland. He has published over 200 Journal and Conference papers and holds three U.S. and one Canadian Patents. He has co-authored, The Six-Port Technique with Microwave and Wireless Applications (Artech House, 2009), and RF Transceiver Design for MIMO Wireless Communications (Springer, 2012). His current research interests include broadband wireless communications, adaptive modulation, MIMO Systems, Mesh and Ad Hoc Networks, Microwave and Wireless Subsystems, Software Design Radio, and advanced wireless transceiver architectures.

Abdolali Abdipour (S'94-M'97-SM'06) was born in Alashtar, Iran, in 1966. He received his B.Sc. degree in electrical engineering from Tehran University, Tehran, Iran, in 1989, his M.Sc. degree in electronics from Limoges University, Limoges, France, in 1992, and his Ph.D. degree in electronic engineering from Paris XI University, Paris, France, in 1996. He is currently a professor with the Electrical Engineering Department, Amirkabir University of Technology (Tehran Polytechnic), Tehran, Iran. He has authored five books and has authored or coauthored over 340 papers in refereed journals and local and international conferences. His research areas include wireless communication systems (RF technology and transceivers), RF/microwave/millimeter-wave/THz circuit and system design, electromagnetic (EM) modeling of active devices and circuits, high-frequency electronics (signal and noise), nonlinear modeling and analysis of microwave devices and circuits.

Mikko Valkama (S'00-M'01-SM'15) received the M.Sc. (Tech.) and D.Sc. (Tech.) Degrees (both with honors) in electrical engineering (EE) from Tampere University of Technology (TUT), Finland, in 2000 and 2001, respectively. In 2002, he received the Best Doctoral Thesis Award by the Finnish Academy of Science and Letters for his dissertation entitled "Advanced I/Q signal processing for wideband receivers: Models and algorithms". In 2003, he was working as a visiting post-doc research fellow with the Communications Systems and Signal Processing Institute at SDSU, San Diego, CA. Currently, he is a Full Professor and Department Head of Electrical Engineering at the newly formed Tampere University (TAU), Finland. His general research interests include radio communications, radio positioning, and radio-based sensing, with particular emphasis on 5G and beyond mobile radio networks.